Turbulent Tube Flocculator, Fall 2014

Felice Chan, Mingze Niu, William Pennock

December 12, 2014

Abstract

Over the fall semester of 2014, the Turbulent Tube Flocculator Team improved the turbulent tube flocculation apparatus in terms of flow control, turbidity control and general structure. The objective of this improvement was to prepare the apparatus by the end of the semester for experimentation. The team made a number of updates this semester, including building a support structure for SWaT and the effluent line. In addition, two air releases were installed as well as a diffuser system in the constant head tank to eliminate air from the flocculator. In addition to the structural modifications of the apparatus, the team updated the process controller method file for experimentation. The experiments performed on this apparatus will be used to validate the equation derived by Dr. Monroe Weber-Shirk based on the experimental work of Dr. Karen Swetland.

Table of Contents

Introduction

The flocculation process is critically important for drinking water treatment, and yet it is only partially understood. Past experimental work by Cornell students working on the AguaClara Project has been performed under laminar conditions. The flocculation done in water treatment plants, like AguaClara designed plants in Honduras, is turbulent, and so it is important to understand the effects of turbulence on flocculation to understand and improve the process. The aim of this research is to improve the existing turbulent tube flocculator apparatus and use it to carry out experiments to gain a better understanding of the flocculation process. The laboratory turbulent tube flocculator is a vertically oriented coiled tube that has a diameter large enough to result in turbulent flow at the experimental flow rate. See Figure 1. The coil is bound by vertical pipe, reinforced with steel bars to create constrictions.

Figure 1: Laboratory Turbulent Flocculator

For the 2014 fall semester, the turbulent tube flocculator team will improve and test the apparatus. The goal is to run a full battery of experiments by the end of the semester. The first step is to design and build a new frame which can fix the **S**ettled **Wa**ter **T**urbidity analyzer (SWaT) at a 60 degree angle. Another important component of making SWaT reliable is to remove air bubbles in the effluent of the flocculator upstream of SWaT. The presence of air

bubbles disrupt the flow in SWaT and can resuspend settled flocs. Air also interferes with turbidity readings. Air will be removed with a vertical standpipe open to the atmosphere just upstream of SWaT.

Because the flow rate in the system is governed by the difference between the elevation of water in a constant head tank and the point where the outlet is at atmospheric pressure, it is necessary to make the elevation of the outlet adjustable so that the flow rate can be readily controlled. An adjustable weir has been designed and added to the apparatus..

As a prerequisite to experiments, the influent turbidity control, which meters clay into the raw water to generate turbidity, needs to be fine-tuned to get steady influent turbidity values. The goal of experimentation is to gather data to explore the applicability of the model proposed by Dr. Monroe Weber-Shirk. This relationship can be seen in the Literature Review section of this report. The experiments will ideally be done in single-day runs that examine the range of settling velocities given an influent turbidity and coagulant dose.Future work will likely explore the role of variation in energy dissipation rate and other model parameters on flocculator performance.

Literature Review

According to the “Flocculation Model” notes developed by Dr. Monroe Weber-Shirk for the CEE 4540 class at Cornell University, flocculation is a process that causes many small particles to aggregate into fewer large particles by means of a chemical coagulant with the aid of adequate mixing. The resultant increase in particle diameters allows the particles to be removed more rapidly by sedimentation. This process is dependent upon the even distribution of an effective coagulant and adequate collisions between coagulant-coated particles. The resulting large particles, known as flocs, are formed as fractals, becoming less dense with increasing diameter (Weber-Shirk).

There are several means of achieving flocculation. One method uses mechanical mixing. In this scheme, the shear necessary for collisions is provided by an impeller powered by a motor. The advantage of this design is that the energy dissipation rate can be varied independently of flow rate, but there is a potential disadvantage with short-circuiting of some fraction of the flow. A more important disadvantage is that the ratio of maximum energy dissipation rate to the average is quite high in mechanical flocculators, yielding inefficient use of the mixing energy and possibly resulting in floc breakup. Beyond flocculation performance, mechanical flocculators require the use of electricity and are prone to mechanical failure of bearings, making them less reliable in places where electric power and replacement parts are difficult to access (Weber-Shirk). Mechanically mixed flocculators are usually far from a plug flow regime, and thus some colloids likely pass through mechanical flocculators without sufficient opportunity to flocculate. Therefore, mechanical flocculators likely require longer residence time to achieve the same performance as hydraulic flocculators. This hypothesis still needs to be tested in a side-by-side pilot study.

Another flocculator type is the hydraulic flocculator. Oftentimes, this is a channel with baffles that cause the flow to alternate direction in a serpentine motion either horizontally (side to side) or vertically (up and down). Alternative configurations of which the team is aware are not practical for municipal-scale treatment. For example, tube flocculators like the ones used in AguaClara research only work for low flows, as readily available tubing does not have sufficient diameter to provide adequate residence time without also incurring considerable head losses. Pipes can also be used for this purpose, but are more expensive to construct than baffled flocculators for a given capacity. Other ideas have included particulate beds, like gravel beds. Without the ability to hydraulically backwash, the operation of these flocculators is intractable. An analogous case is that of porous substances, like reticulated foam, which cannot be disassembled for cleaning. Also, at small enough pore sizes, the above two cases (gravel and foam) approach filtration, which both enhanced mixing and storage of particulate matter. Storage of particles makes the flocculator more reliant on backwash and causes it to operate further from continuous steady-state operation. Nonetheless, particulate beds with sizes small enough to fluidize could be useful. Preliminary research has indicated that highly fluidized beds of particles less than 100 μm might be able to serve as flocculators (fluidized bed flocculation).

Although hydraulic flocculators have hydraulic advantages (e.g., uniform mixing) and operational advantages (e.g., no moving parts), they are less frequently used as their design is poorly documented and their use has little economic incentive for equipment vendors due to its lack of requisite proprietary parts. The AguaClara Program, however, has used hydraulic flocculators to great effect as demonstrated by nine operational plants in Honduras. Nevertheless, AguaClara recognizes the need the understand the fundamental physics underlying the process so that hydraulic flocculator designs can be made more physically based (Weber-Shirk).

Attempts to better understand flocculation at Cornell University have been based on the experimental work of Karen Swetland. A model was fit to her results. As her results were obtained with a reactor in the laminar regime, it is not expected that this model will apply to the turbulent conditions present in municipal-scale flocculators (Weber-Shirk). As Cleasby observed, at scales larger than the Kolmogorov length scale in turbulent flows, $\varepsilon^{2/3}$ is a more appropriate flocculation parameter than G, which is appropriate at scales smaller than the Kolmogorov length scale (1984).

The turbulent flocculation model posited by Dr. Weber-Shirk is analogous to the laminar model and takes the form:

$$pC^* = \frac{9\log(e)}{8} W\left(\frac{8}{9}\Gamma\varphi_0{}^{8/9}\frac{t\varepsilon^{1/3}}{d_{colloid}{}^{2/3}}\frac{\eta_{coag}}{V_{capture}}\right) \qquad (1)$$

where pC^* is the negative logarithm of effluent turbidity over inlet turbidity, W is the Lambert W function, Γ is the fractional coverage of coagulant on particles, φ_0 is the initial floc volume fraction, ε is the energy dissipation rate, t is time, $d_{colloid}$ is the diameter of primary particles,

$V_{capture}$ is the capture velocity in sedimentation, and η_{coag} is a fitting parameter relating to the performance of the coagulant in the units of settling velocity (Weber-Shirk).

In continuing this work, it is useful to examine past work on turbulent flocculation. In 1984, Cleasby observed that there was little work done on flocculation, and that more was needed (Cleasby 1984). Since that time, additional work has been performed, including a study by Leonard W. Casson and Desmond F. Lawler using an oscillating grid flocculator (Desmond and Lawler 1990).

In this study, flocculation with the oscillating grid was conducted under two conditions, a grid moving at 0.25 Hz with an amplitude of 0.75 in, and a grid moving at 0.75 Hz with an amplitude of 0.25 in. Hydraulic studies indicated that there were eddies at several scales created by these conditions. While larger eddies were different between the two conditions, the smallest eddies (< 100 μm) were nearly identical between them. The advantage of using an oscillating grid reactor is that there is finer control of the characteristics of small eddies compared with other reactors. Most flocculators induce large eddies that are then dissipated to small eddies, whereas this study created small eddies directly and large eddies indirectly. The authors hypothesized that if flocculation performance were different between the two conditions, it could be attributed to the larger eddies, which would indicate that larger eddies control flocculation performance. Conversely, if the performances were similar, it could be concluded that flocculation performance depends on small eddies (Casson and Lawler 1990).

The authors conducted experiments on monodisperse, bimodal, and trimodal distributions of 2.02, 5.9, and 21.1 μm particles, all at densities of 1.05 g/cm^3. The results of these studies showed little difference in performance between the low amplitude, high frequency condition and the high amplitude, low frequency condition, leading the authors to conclude that flocculation performance is dependent upon eddies that are close to the size of the particles being flocculated. They infer that energy spent creating large eddies is wasted except in keeping particles suspended (Casson and Lawler 1990). While this is not an unfounded conclusion, it may not be sufficiently nuanced. The authors did not note the importance of the distance between colliding particles. Researchers in the AguaClara program have observed that it is the average distance between particles that sets the effective eddy size for creating collisions. Casson and Lawler, on the other hand, considered the summative volumes of the colliding flocs as determining the volume of eddy that facilitates flocculation.

An interesting result of the experiments carried out by of Casson and Lawler was that particles of different sizes in the bimodal and trimodal distributions were found to have negligible effect on each other. That is, the presence of larger particles in the bimodal distribution did not give an improvement in performance over the case with a monodisperse distribution of small particles. The sizes appeared to flocculate independently of each other (Casson and Lawler 1990).

Based on their findings, Casson and Lawler refined a model that had been previously developed for turbulent flocculation by Adler (1981) as well as Valioulis and List (1984) based upon the original formulation by Smoluchowski (1917). The modified model is as follows:

$$\frac{dn_k}{dt} = \tfrac{1}{2}\alpha_c \sum_{i+j=k} \alpha(i,j)\beta(i,j)n_i n_j - \alpha_c n_k \sum_{i=1}^{q} \alpha(i,k)\beta(i,k)n_i \qquad (2)$$

where, "$i,j,$ and k are subscripts denoting particle size, q is the maximum allowable value of $i,j,$ or k in the model, n is the number concentration of the particles (cm^{-3}), t is time(s), $\beta(i,j)$ is the collision frequency function (cm^{-3} s^{-1}), $a(i,j)$ is the size-dependent collision efficiency factor resulting from the hydrodynamic effects on particle interaction, and α_c is the chemical collision efficiency factor accounting for other interactions (Casson and Lawler 1990). The variable $\beta(i,j)$ is defined as the following function (Casson and Lawler 1990):

$$\beta(i,j) = \tfrac{1}{6}(d_i + d_j)^3 G \qquad (3)$$

where "d_i and d_j are diameters of particles of sizes i and j, respectively (cm), and G is the root-mean-square (RMS) velocity gradient (s^{-1})" (Casson and Lawler 1990).

It is noteworthy that the above model, like the model built on Swetland's work does not include floc breakup. More recent studies have developed population balance models that incorporate both aggregation and breakage, and a number of these are summarized in Kumar, et al. (2009).

There are a number of noteworthy differences between the AguaClara flocculation model and that proposed by Casson and Lawler. Firstly, the AguaClara model is presented as an integral relation that can be directly solved. The Lawler and Casson model, however, is a differential model, which may not have a closed-form solution, depending on the summation terms contained within it. The presence of the β term in the Lawler and Casson relation appears to express the authors' assertion that the sum of the volumes of particles being flocculated is the quantity that controls the size of eddy that is effective in flocculation. Meanwhile, the presence of φ in the AguaClara model reflects the importance of distance between particles. This is distinct from the n terms in the Casson and Lawler model, as these only account for the absolute number of particles, and not their relative volumetric contributions. The Casson and Lawler model ultimately solves for the change in absolute number of particles, while the AguaClara model is concerned with the concentration of nonsettleable particles. The AguaClara model also contains a few parameters that do not appear in the Casson and Lawler model. The Γ and η_{coag} terms account for the coverage and performance of the coagulant, which might be accounted for in α_c in the Lawler and Casson model. It is not clear that the effects contained in $\alpha(i,j)$ are included in the AguaClara equation. Another interesting difference is that Lawler and Casson include G ($\sqrt{(\varepsilon/\nu)}$) in the $\beta(i,j)$ function which would be correct for laminar flow flocculation, while the AguaClara model uses $\varepsilon^{\frac{1}{3}}$ to account for the role of turbulent eddies in providing collisions. Lastly, the

AguaClara equation considers the impact of sedimentation to predict the settled water turbidity with the inclusion of $V_{capture}$. The Lawler and Casson equation does not make any predictions about settled water turbidity.

Moving to the design of the apparatus, the scheme used to control the influent turbidity is known as Proportional-Integral-Derivative (PID) control, which is the most ubiquitous industrial control scheme. It works by comparing a monitored value to a target value and adjusting accordingly. PID control compares readings to the target value in three ways.The proportional component evaluates the magnitude of the difference between the instantaneous measured value and the target value. Likewise, the integral component evaluates the sum of errors (difference from target value) over time. Lastly, the derivative component measures the rate at which the value is changing, and attenuates unfavorable changes. The control scheme comprises the net response generated by these components. In this case of this apparatus, PID compares readings from the influent turbidimeter to a target turbidity value (50 NTU). These readings are taken by an online turbidimeter which is connected to a closed loop that flows out of and back into the raw water stock tank by means of a peristaltic pump. The comparison is then used to control the peristaltic pump that adds a clay suspension into the raw water stock tank. For this project, only the proportional (P) and integral components (I) are used, and these will need to be adjusted to maintain stable values of influent turbidity (PID, 2011).

Previous Work

The turbulent tube flocculator was designed by the Summer 2013 team by setting a target Reynolds number of 4000 and a target energy dissipation of 30 mW/kg to ensure turbulent conditions. The general design that was decided upon is a vertically coiled tube with a series of constrictions. The equations for flocculator design obtained from the flocculation design notes from CEE 4540 were modified for a circular geometry, as opposed to a rectangular geometry, in order to create a coiled flocculator for lab scale research.

The height to spacing ratio, or the H/S ratio will determine the dimensions of the tubing for the flocculator and influence the spatial efficiency of mixing in the flocculator. For a baffled flocculator, the height is typically defined as the depth of water, and the spacing is defined as the space between the baffles. Because the equations for flocculation design were modified for a circular geometry, the definition of H becomes the distance between the constrictions in the tube and the spacing is the inner diameter of the tubing. For an H/S ratio that is greater than 5, there is some amount of distance before the next baffle with very low energy dissipation that does not contribute much to flocculation, and therefore an H/S ratio of approximately 5 is desirable. The design parameters shown in table 1 were used to design the rest of the flocculator.

Table 1: Design Parameters for Turbulent Flocculator

Design Parameter	Symbol	Value
Reynolds Number	Re	4000
Energy Dissipation Rate Coefficient for Jets	Π_{Jet}	0.225
H/S Ratio	Π_{HS}	5
Head loss coefficient for a baffle	K_B	2
Viscosity of Water	v	1 mm^2/s
Energy Dissipation Rate	ε	30 mW/kg
Thickness of Tubing Wall	T_{wall}	⅛ in

To determine the minimum inner diameter of the tubing, equation 4 was used. Using the desired energy dissipation rate of 30 mW/kg, the inner diameter calculated was 3.039 cm (1.196 in). Using the calculated inner diameter, the width of the constrictions was determined to be 1.117 cm (equation 5). To find the spacing between the constrictions on the flocculator, the inner diameter of the tube was multiplied by 5 to yield a spacing of 15.197 cm (but 16.07 cm was used).

$$ID_{tube} = \left[\frac{(Re \bullet \nu)^3 K_b}{\Pi_{HS} \bullet \varepsilon_{tube}}\right]^{1/4} \qquad (4)$$

$$H_{tube} = \frac{1}{5}(5ID_{tube} - \sqrt{10}ID_{tube}) \qquad (5)$$

Equation 6 was used to determine the required flow rate of the flocculator, which is 95.484 mL/s.

$$Q_{plant} = \frac{\pi}{4}\left[\frac{(Re \bullet \nu)^7 \bullet K_b}{\Pi_{HS} \bullet \varepsilon_{tube}}\right] \qquad (6)$$

To find the collision potential per baffle, equation 7 was used. This required a determination of the number of constrictions required. The collision potential per baffle is 0.285 $m^{2/3}$, and therefore, the number of constrictions is the total collision potential divided by the collision potential per baffle, which is 351 constrictions (equation 8). The length of the flocculator is determined by multiplying the number of constrictions by the length of the spacing (equation 9). The total length of the flocculator is 56.353 m.

$$\psi_c = \left(\frac{\Pi_{jet}^3}{2\Pi_{VC}^4}\right) K_b^{1/3} H_{spacing}^{2/3} \qquad (7)$$

$$N_{Constraint} = \frac{\psi}{\psi c} \qquad (8)$$

$$L_{floc} = H_{Spacing} \bullet \left(\frac{\psi}{\psi_c}\right) \quad (9)$$

The hydraulic residence time per spacing between collisions can be calculated using equation 10. Therefore, the total hydraulic residence time for the flocculator is the product of the residence time per baffle and the number of constrictions (equation 11). Therefore, an estimate of the residence time of the flocculator is 7.546 minutes.

$$\theta_c = \frac{H_{Spacing} ID^2}{Q^4} \quad (10)$$

$$\theta_{Floc} = \theta_c \left(\frac{\psi}{\psi_c}\right) \quad (11)$$

To find the diameter of the coiled flocculator, equation 12 was used. To find the number of coils, the length of the flocculator was divided by the product of the spacing and the number of constraints per coil (equation 13). The minimum diameter of the flocculator is 0.58 m (0.614 m was actually used), and the number of coils required is 30.

$$D_{Coil} = \frac{H_{Spacing} N_{ConstPerCoil}}{\pi} \quad (12)$$

$$N_{Coil} = \frac{L_{Floc}}{H_{Spacing} N_{ConstPerCoil}} \quad (13)$$

To find the total height of the system, the number of coils was multiplied by the sum of two times the wall thickness plus the constricted height of the tube, to yield 1.464 m (equation 14).

$$H_{System} = N_{Coil} * (H_{tube} + 2T_{Wall}) \quad (14)$$

A summary of all the calculated flocculator parameters is shown in table 2.

Table 2: Calculated Flocculation Dimensions and Parameters

Parameter	Value
Reynolds Number (Re)	4000
Inner Diameter of Tubing (H)	0.0318 m (1.25 in)
Energy Dissipation Rate (ε)	30 mW/kg
Collision Potential (ψ)	100 $m^{2/3}$
Length of Flocculator (L)	55.315 m
Number of Coils	30
Diameter of Coils	0.614 m

Constricted height	1.464 m
Hydraulic Residence Time (θ)	7.005 min

Because of calculation error when designing the flocculator, table 3 shows the actual dimensions that were used to construct the flocculator. (The Summer 2013 team had designed the entire with a Π_{HS} of 4 but used a Π_{HS} of 5 when calculating the spacing between the baffles.)

Table 3: Actual Flocculation Dimensions and Parameters

Parameter	**Value**
Reynolds Number	4000
Inner Diameter of Tubing	0.0318 m (1.25 in)
Energy Dissipation Rate	30 mW/kg
Collision Potential	100 $m^{2/3}$
Length of Flocculator	56.35 m
Number of Coils	30
Diameter of Coils	0.614 m
Height of Flocculator	1.464 m
Hydraulic Residence Time	7.546 min

The Fall 2013 and Spring 2014 team worked on the fabrication of the flocculator, and designing and constructing other parts of the apparatus necessary to run experiments.

1. Head Tank Volume: To ensure an accurate influent turbidity, the minimum head tank volume for the system was determined based on the response time of the turbidimeter. Using a 5 gallon tank is appropriate because the minimum volume required is 1.6 gallons.

$$t_{turbidimeter} = \frac{V_{Sample}}{Q_{turbidimeter}} = \frac{30\ mL}{5\ mL/s} = 6\ s \quad (15)$$

$$V_{HeadTank} = Q_{Plant} \cdot (10 \cdot t_{turbidimeter}) = 6.06\ L = 1.6\ gal \quad (16)$$

2. New Solenoid Valves: New solenoid valves were purchased to accommodate the high flow rate required. The orifice diameter is 5/32 of an inch and the pipe size is ¼ of an inch.

3. Rapid Mix Unit: The target energy dissipation rate is 1 W/kg, and therefore the diameter of the orifice is 1.87 cm.

$$D_{Jet} = \left(\frac{4Q_{Plant}\Pi_{Jet}}{\varepsilon^{1/3}\pi}\right) \quad (17)$$

$$D_{Orifice} = D_{Jet}\frac{1}{\sqrt{\Pi_{VC}}} \quad (18)$$

4. Tube Settler: The minimum spacing to prevent floc rollup is 2.5 cm, or 0.984 in, so the chosen diameter of the tube settler was 1 in. The formula for capture velocity is given by equation 15, where S is the spacing between the plates (or inner diameter of the tube), L is the length of the tube, V_{plate} is the vertical velocity through the tube and alpha is the plate angle, which was set at 60 degrees. Using a target capture velocity of 0.12 mm/s, the length of the tube settler was calculated to be 86 cm and the flow rate through the tube settler is 1.002 mL/s from equation 16.

$$V_{Capture} = \frac{S \cdot V_{Plate}}{L \cdot sin(\alpha) \cdot cos(\alpha) + S} \quad (20)$$

$$Q_{tube} = A_{tube} \cdot \frac{V_{Capture} \cdot (L_{tube} sin(\alpha) cos(\alpha) + D_{Tube})}{D_{tube}} \quad (21)$$

Methods

Current Apparatus

A simple schematic of the experimental apparatus is shown in Figure 1. It demonstrates the major components of the apparatus, which are: the flocculator, the clay stock tank and pump, the raw water stock tank, the temperature and pressure controls, and the coagulant stock bottle and pump. Water is supplied to the raw water stock tank from two sources: hot water and cold water. The flow of these into the raw water stock tank is regulated by two solenoid valves that ensure that the water level in the stock tank remains constant and that the temperature of the water remains close to ambient temperature in the laboratory. Flow through the apparatus is controlled by the difference in height between the height and the height at which the effluent from the flocculator is at atmospheric pressure (represented as Δh in the figure). As will be shown, this height can be adjusted in order to provide control over the flow rate.

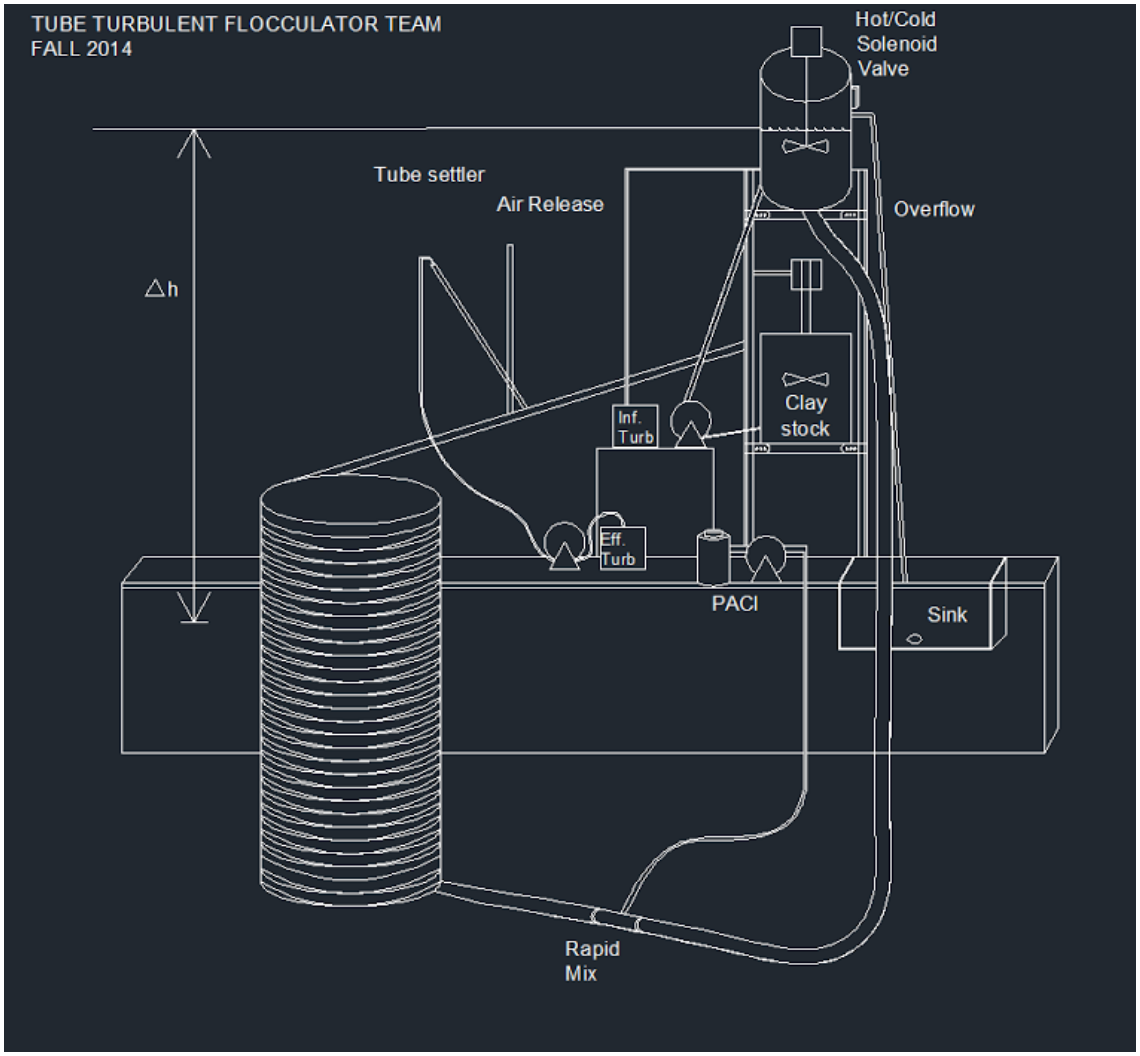

Figure 2: AutoCAD Drawing of Current System

Process Controller Update

A new function “Water Temperature- Depth Control” was incorporated into the current method file. This feedback control was used for the hot and cold solenoid valves to monitor the temperature and the depth of water in the head tank in one state. The Water Temperature- Depth control function also matches the water temperature to the air temperature in the room to prevent density currents in the tube settler.

Currently, the only two states in the method file are “off” and “running”. The cold solenoid valve will turn on if and only if the temperature of the water is greater than the air temperature and the current water level is less than the maximum water level. Similarly, the hot solenoid valve will turn on if and only if the temperature of the water is less than the air temperature and the water level in the tank is less than the maximum water level. These relationships are summarized in figure 1.

The new process controller file allows for the creation of new states that cycle the flocculator through different coagulant doses while maintaining the raw water reservoir.

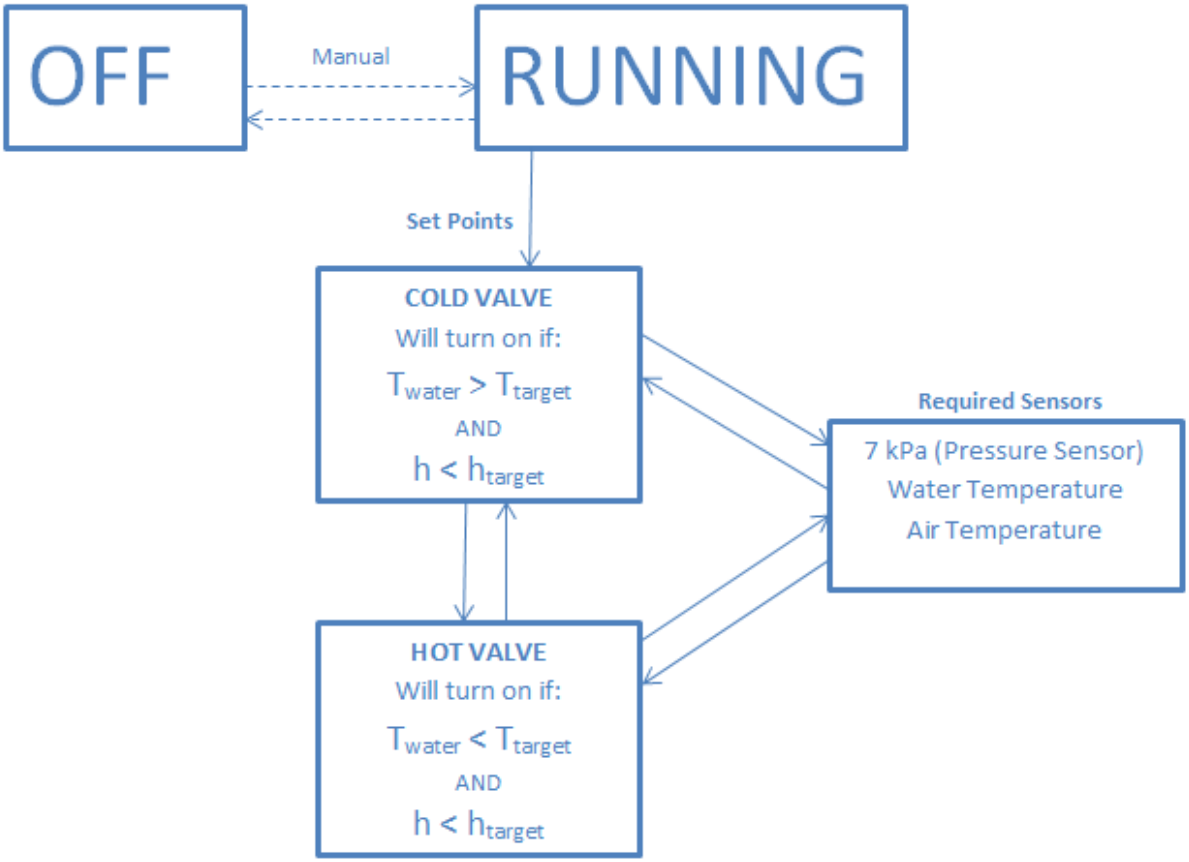

Figure 3: Process Controller Method File Schematic

Modification of Apparatus

In order to remove the ad hoc implementation of a ring stand as a tube support, a horizontal 80/20 bar was added as a span between the 80/20 stock tank stand and the top of the flocculator. This serves as the new structural support for the outlet. With the use of zip ties, the outlet line, which is partly constructed of flexible tubing, was affixed to the horizontal bar to keep it from sagging and kinking. There are two T-tubes attached on the outlet tube; one is used for air bubble removal, and the other is a settler for the Settled Water Turbidity (SWaT) analyzer, which is fixed at a 60° angle to the horizon. There is also a support frame attached to the horizontal bar, which allows the SWaT settler to have an adjustable angle.

There is an inline air release tube installed prior to the SWaT tube, which is used to remove air bubbles from the flow prior to entering the SWaT tube. It is open to atmospheric pressure to allow the bubbles to escape.The air release prevents the air bubbles from coming into the SwaT tube, which ensures that the particles settled at the bottom of the tube are not

disturbed by air bubbles, which is important when running the experiment. It also keeps air from entering the turbidimeter, since bubbles can alter turbidity readings.

Another main modification has been made to the effluent drain. Since the height difference between the water level in the constant head tank and the height at which the effluent from the flocculator reaches atmospheric pressure determines the flow rate, the height at which the effluent drain enters free fall (atmospheric pressure) has been made adjustable. This has been done by connecting the drain to a slider on the stock tank frame. This slider has an air release to ensure that atmospheric pressure is reached at the elevation of the slider and that freefall will begin at that point. The drain is connected to the slider by means of flexible tubing to make the height more easily adjustable. A diagram of this system is provided in Figure 5. To achieve a flow rate of 95 mL/s, the team adjusted the height of the effluent drain to be 28 cm below the overflow drain on the constant head tank.

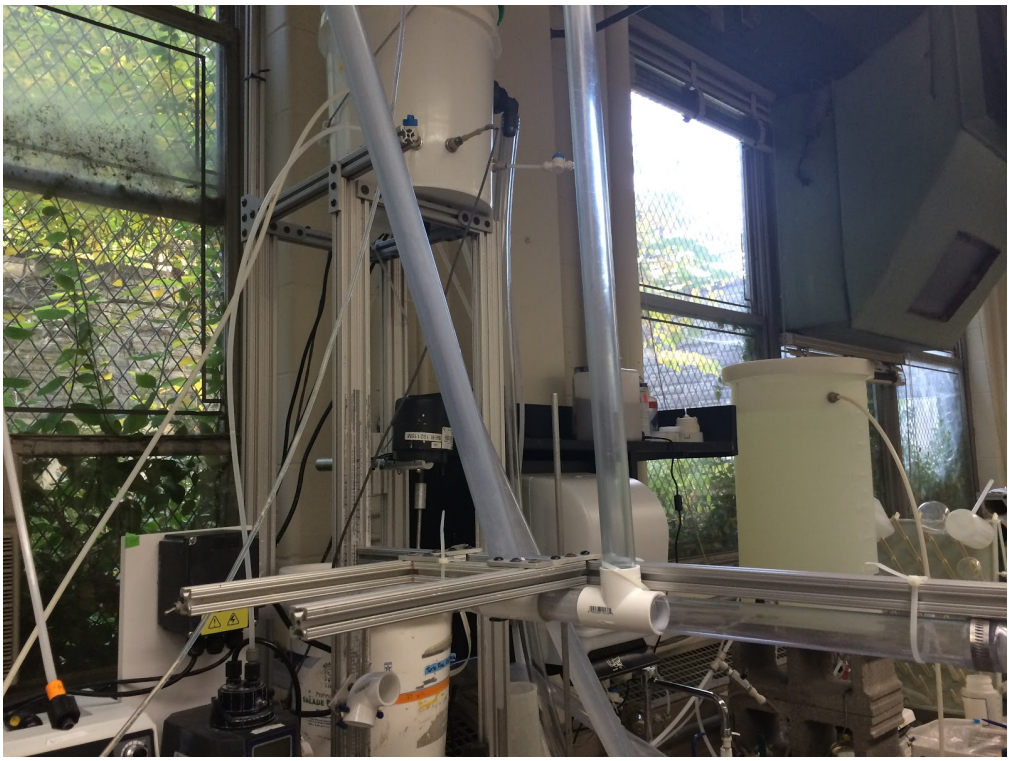

Figure 4: Photograph of modification of apparatus

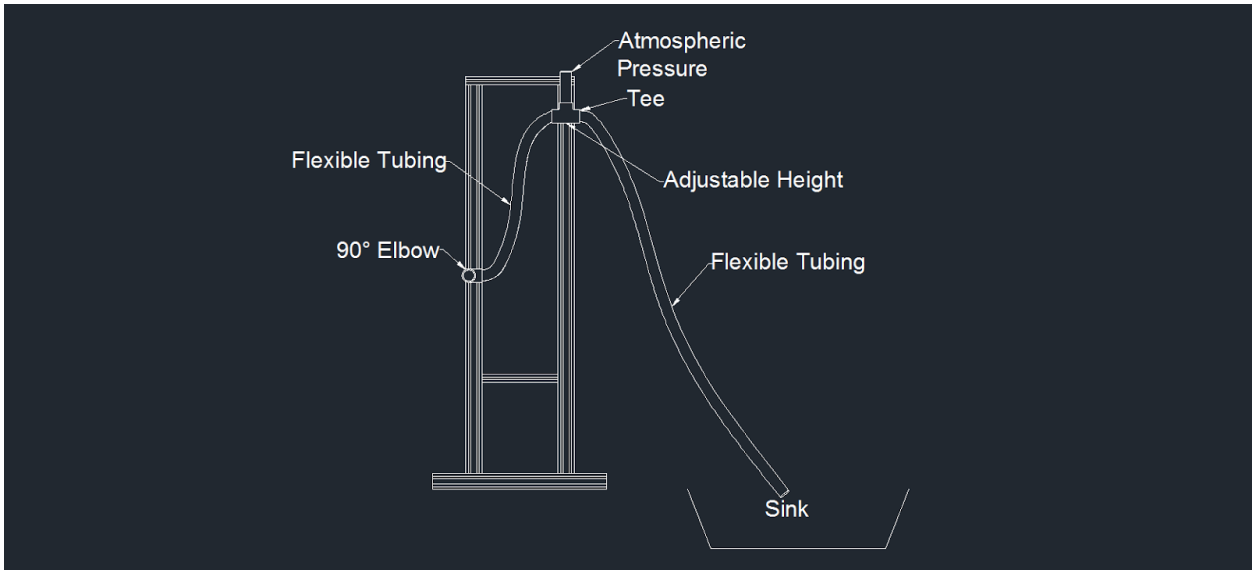

Figure 5: Design Diagram of Adjustable Elevation Drain

Clay Dosing System

The team tried to replace the tubing for the clay dosing systems with microbore tubing with size 13 peristaltic pump tubing to prevent clay from setting in the tube. However, with a tubing size this small, the team would need a clay stock concentration of 170 g/L, which would not be feasible. Therefore, the team switched the tubing to size 16 peristaltic pump tubing, which requires a clay stock of 12 g/L.

Pulse Input Tracer Test

In order to better understand the hydraulics of the flocculator, the team first performed a pulse input tracer test with red dye #40. This allowed the team to experimentally determine the hydraulic residence time of the system and verify the residence time calculations. The team injected 10 mL of 10 g/L red dye solution directly into the entrance tube using a funnel and flexible tubing, and then measured the time for the leading edge of the dye to exit the system. The dye test can be treated as a pulse input to a plug flow system with some dispersion. When the dye was initially injected, the leading and trailing edges were very distinct and became increasingly faint as the slug traveled through the flocculator, indicating the effects of dispersion.

Figure 6: Red Dye flowing through floccuator. The head and tail are becoming faint by this point in the flocculator, implying dispersion.

However, this is not an accurate measurement of hydraulic residence time because the flow rate of the plant must be adjusted to the desired flow rate of 95 mL/s. At the time of this test, the flow rate of the system was measured to be approximately 200 mL/s, twice the desired flow rate, because the effluent drain was too low in relation to the water level. Additionally, the original calculation for residence time only considered the body of the flocculator, not the entrance and exit tubes. The hydraulic residence time that the team measured was 6 minutes and 20 seconds, including the inlet and outlet tubes.

In order to perform a more accurate pulse test to measure hydraulic residence time, the team chose to use clay instead of dye as a tracer. This allowed the team to take instantaneous on-line measurements of the effluent concentration by means of a turbidimeter. The results for one such experiment are shown in Figure 7, below. In this pulse test, a 30 mL slug of a 10 g/L clay suspension was inputted into the influent of the turbidimeter by means of a turkey baster. The peak concentration occurred about 8 minutes, 30 seconds after the pulse input. This is in good agreement, with the theoretical residence time of the system:

$$\theta = \frac{L}{v} = \frac{L}{Q/A} = \frac{LA}{Q} = \frac{60\ m(\pi\frac{(31.75\ mm)^2}{4})}{95\ mL/s} = 8.33\ min$$

The above pulse input test gives reasonable confidence that the residence time in the flocculator is as predicted. The data suggest that the turbulent tube flocculator is a plug flow reactor with some dispersion.

The team performed an analysis to find the exit age distribution, E(t), the cumulative age distribution, F(t), and, D, the sum of the dispersion and diffusion coefficients. The dimensionless term D/v_xL represents the single parameter of the model, referred to as the dispersion number, which gives the relative measure of the importance of dispersion and advection in the mass balance equation. The larger the dispersion number, the more significant dispersion is relative to advection (Benjamin and Lawler 2013).

The team converted the effluent turbidity readings in NTU to mg/L by using the conversion factor of 1.7. E(t) can then be computed using equation 22, where Q is the plant flow rate, $M_{p,in}$ is the mass of tracer added, and $c_p(t)$ is the concentration in mg/L.

$$E(t) = \frac{Q}{M_{p,in}} * c_p(t) \qquad (22)$$

The exit age distribution is plotted in figure 8. Typically, this has the same shape as the effluent tracer concentration, but for the purposes of this analysis, the zero level of concentration has been adjusted to eliminate the effect of background turbidity which was at a constant concentration of approximately 10 NTU. In addition, t=0 was set as to the time where the concentration started to increase. The cumulative age distribution F(t), can be obtained by numerically integrating E(t).

The sum of the dispersion and diffusion coefficients can be computed from equation 23, where σ^2_{RTD} is the variance residence time distribution, $\bar{t}$ is the mean residence time, v_x is the mean velocity in the x direction, and L is the length of the reactor.

$$\frac{\sigma^2_{RTD}}{\bar{t}} = \frac{2(D/v_xL)+8(D/v_xL)^2}{\{1+2(D/v_xL)\}^2} \qquad (23)$$

From this equation, D was determined to be 1.0145×10^6 cm^2/min, and D/v_xL is 0.242 which corresponds to a Péclet number of 4, meaning the process is advection dominated with some effects of dispersion.

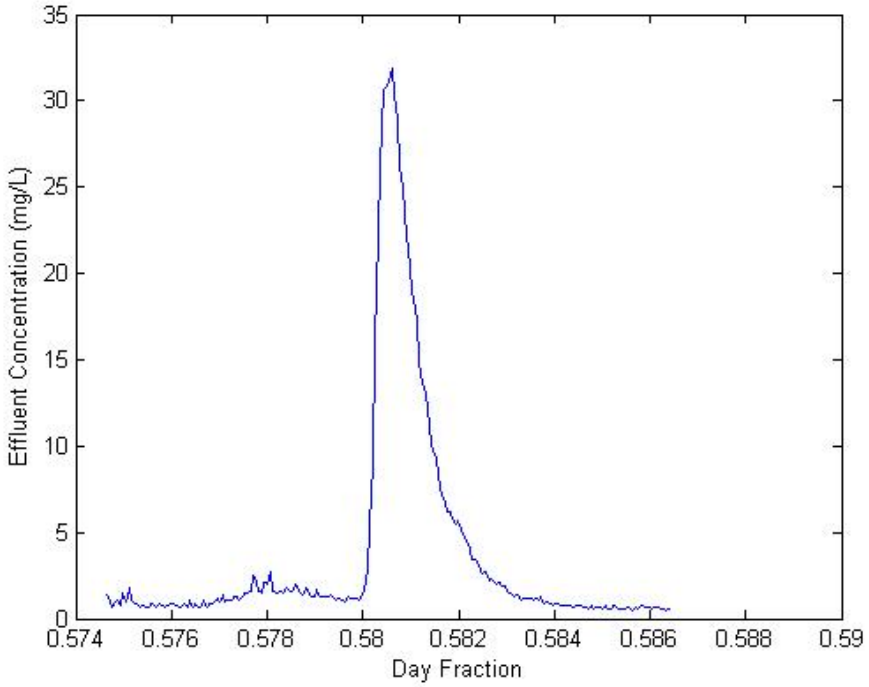

Figure 7: Effluent Concentration for Pulse Input Test

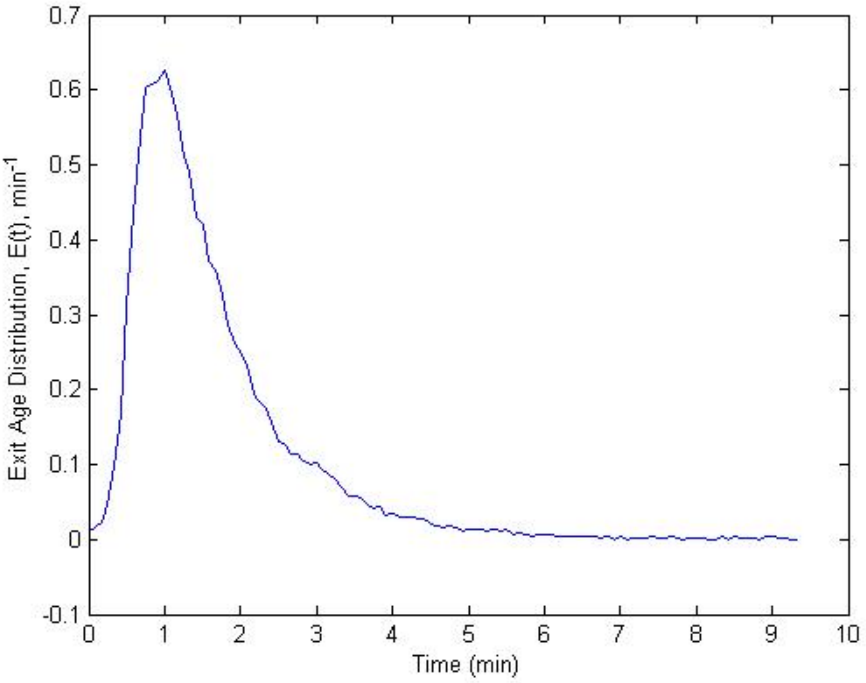

Figure 8: Exit Age Distribution

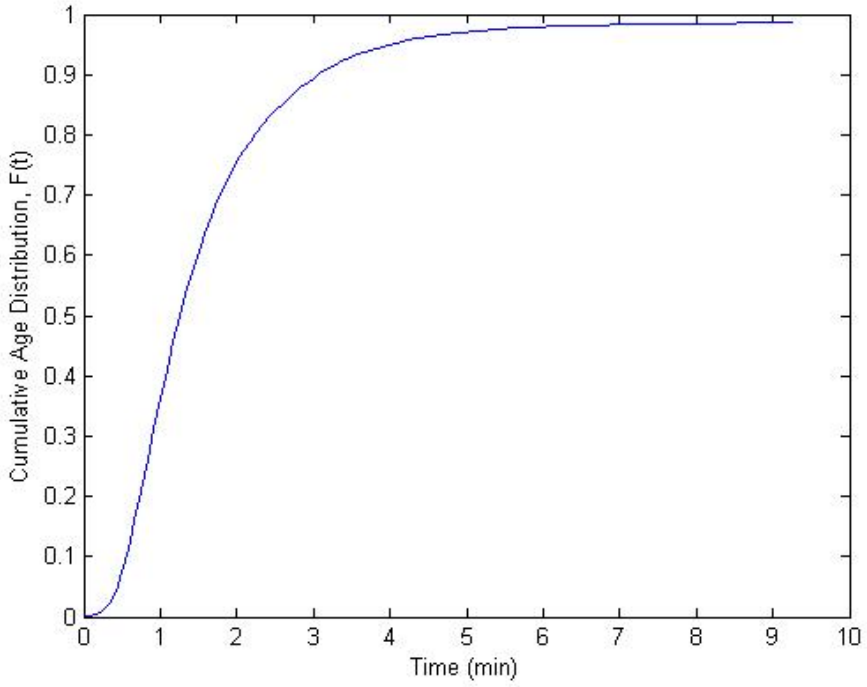

Figure 9: Cumulative Age Distribution

Air Stripping Unit

Particularly during the winter months, dissolved air poses a considerable challenge to water experiments in Ithaca. The water source is equilibrated with air at cold temperatures, which make air more soluble. When this water is exposed to higher temperatures in laboratory settings, it exits the solution and forms bubbles due to the higher volatility of gases at higher temperatures. These bubbles are problematic, because they interfere with nephelometric turbidity measurements, leading to overestimates of turbidity. To mitigate this problem, the team installed four diffusers into the constant head tank as shown in Figure 7. These bubble air into the solution so that dissolved gas can transfer out of solution before entering the apparatus. This addition was demonstrated to significantly reduce the presence of dissolved air, but not completely. This could possibly be because the flow rate through the system is currently higher than the design flow rate. At the design flow rate, the residence time for the stock tank may be sufficient for the air stripping process to proceed to a satisfactory level. If it is found that the diffuser system is still inadequate after the flow rate is lowered, the team may need to consider other alternatives, such as changes to the stock tank design.

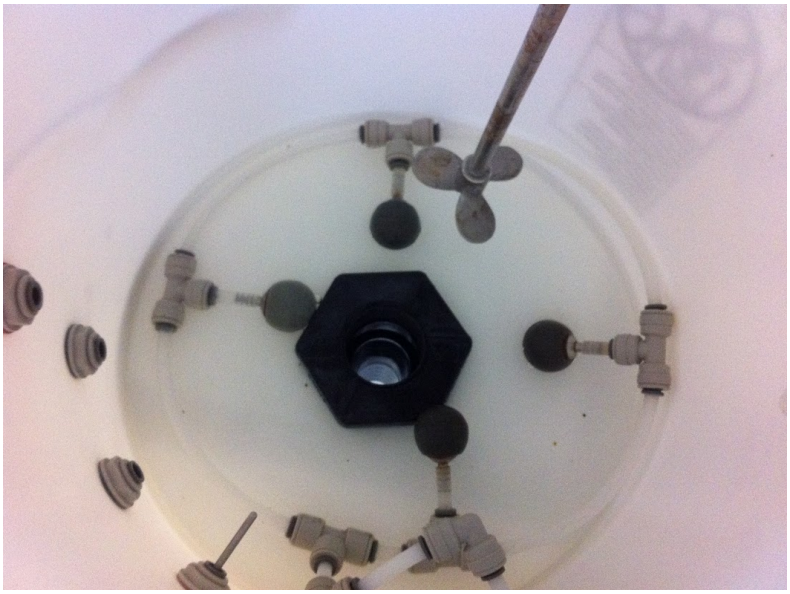

Figure 10: Diffuser System in Stock Tank

Results and Discussion

To date, there are still some problems with the process controller method file and the apparatus. For example, PID, which is controlling the influent turbidity, is still allowing the influent turbidity to fluctuate between 48 and 52 NTU. Further calibration of the PID controller is still needed.

Before full experimentation can begin, the coagulant pump must be recalibrated to ensure that it is pumping the appropriate dose each time. Likewise, the SWaT pump must also be properly calibrated to provide adequate settling time in SWaT. In a few trials, the pump for the SWaT system was pumping a flow rate that was approximately 1/7th of the desired flow rate which indicated a hydraulic residence time of approximately 49 minutes as opposed to the calculated SWaT residence time of 7 minutes. As these experiments were only half an hour long, the data were not considered valid, given the extremely long residence time in SWaT. The team has now successfully calibrated the pump so that the appropriate flow rate of 1.002 mL/s is flowing through SWaT.

The team also noticed that there is settling throughout the entire body of the flocculator, including the length of tubing connecting the constant head tank to the rest of the flocculator and the exit tubing, which is where SWaT draws from. Thus, there is a high turbidity flow in the lower half of the tube and a clarified flow in the upper half of the tube, as shown in figure 11. Because the SWaT system is drawing water from the top of the tube, the effluent turbidity is likely an underestimate of the true value. The settling in the entrance tubing was resolved by lifting the tube and letting the clay fall through into the rest of the system, but this method of reincorporating the clay into the system is not practical on a

long-term basis. A potential solution for the leading end of tubing would be to shorten it to eliminate the length of tubing that is just resting on the ground. However, for the main body of the flocculator and the length of tubing leaving the flocculator this is impossible because the tubing is clamped together in the body of the flocculator, and the tubing exiting the flocculator is rigid.

The team ran an experiment with a target influent turbidity of 50 NTU with no coagulant. The average effluent turbidity was 40 NTU, which implies that the 10 NTU difference was due to clay settling and sticking to the walls of the flocculator. Potentially, the team could run a slightly acidic solution through the flocculator to try to remove some of the clay and coagulant that has stuck and settled to the sides of the flocculator.

Figure 11: Clay Settling in Flocculator Effluent Tube

Future Work

Having finished the above modifications, the sub-team is in the process of calibrating the PID control for influent turbidity in order to make influent turbidities in the system stable. After these final touches, the apparatus will be essentially ready to run experiments, but will require some further testing as well as further development the method file for experiments in Process Controller. At present, the plan is to vary coagulant dose, influent turbidity, and capture velocity. For these experiments, the parameters will be arranged in a hierarchy, such that each turbidity is tested at a range of coagulant doses, which are then tested at varying settling velocities. That is to say that the hierarchy of parameters will be coagulant dose, then influent turbidity, then capture velocity. Influent turbidities will be varied between 5, 15, 50, 150, and 500 NTU. Capture velocities will be varied between 0.06, 0.12, 0.25, 0.5, and 1.0 mm/s. There is currently some uncertainty about what constitutes an adequate coagulant dose, as each influent turbidity value will have a different range of coagulant doses that are effective. As a baseline, the Summer 2014 research on laminar flocculation used coagulant

doses that proved excessive, so these will be considered maxima for the doses this research will use.

The purpose for the initial experiments is to determine the coagulant dose values at which, for a given turbidity and settling velocity, the response of performance (pC^*) to increased coagulant dose changes. This will be analyzed graphically on plots with pC*as the ordinate, and $\Gamma\varphi_0{}^{8/9}\frac{t\varepsilon^{1/3}}{d_{colloid}{}^{2/3}}$ as the abscissa. The dependent variable on the abscissa increases with coagulant dose, since the fractional coagulant coverage (Γ) increases with increased dose. From laminar studies by Swetland, it is anticipated that there will be two points at which the response of the performance changes. The first is at the beginning when coagulant has been added and flocculation is beginning but has not yet produced settleable flocs. Initially, there is no response on pC*, and this is referred to as the first phase. The second phase begins at coagulant doses sufficient for particle aggregation and removal by settling. In this region pC* is expected to increase linearly with coagulant dose. When the coagulant reaches a certain point, neither pC^* nor $\frac{9\log(e)}{8}W(\frac{8}{9}\Gamma\varphi_0{}^{8/9}\frac{t\varepsilon^{1/3}}{d_{colloid}{}^{2/3}}\frac{\eta_{coag}}{V_{capture}})$ increase, because, at this stage, maximum colloid surface coverage has been attained ($\Gamma = 1.0$). As a result there is no change in pC* when the coagulant dose increases. This is the third phase, and is marked by a locus of points at the point where the second phase ends. It is essential to the model to find out where these three phases occur. It is also possible that floc breakup becomes significant when the settled water turbidity is very low. This may show up as a plateau in the data at high values of $\Gamma\varphi_0{}^{8/9}\frac{t\varepsilon^{1/3}}{d_{colloid}{}^{2/3}}$ Initial experiments will analyze a minimum of seven coagulant doses for each experimental condition, with finer variations in concentration used later to find the exact coagulant doses that correspond to transitions between phases.

The Process Controller file for these experiments will take a constant value of influent turbidity. This value of turbidity will be used for seven experiments that will each use one of seven different coagulant doses. Each experiment at a given influent turbidity and coagulant dose will use five different capture velocities. In total, there will be five of these sets of seven experiments, one set for each value of influent turbidity. Thus, there will need to be $5 \times 7 = 35$ sets of experiments ($5 \times 7 \times 5 = 175$ different conditions) run. The times for these experiments will be non-trivial, as the residence time of the flocculator is about 7 minutes and the minimum residence time of the SWaT settler is 1 minute $(\theta = \frac{L}{v} = \frac{860\ mm}{17.004\ mm/s} = 50.6\ s)$. The longest SWaT retention time is about 14 minutes $(\theta = \frac{L}{v} = \frac{860\ mm}{1.02\ mm/s} = 843.1\ s = 14.1\ min)$.

References

Adler, P.M. (1981). Heterocoagulation in Shear Flows. Journal of Colloid & Interface Science,
83:1:106

Benjamin, M., & Lawler, D. (2013). Continuous Flow Reactors: Hydraulic Characteristics. In Water quality engineering: Physical/chemical treatment processes (1st ed., pp. 33-54). Hoboken, NJ: John Wiley & Sons.

Casson, L. W., & Lawler, D. F. (1990). Flocculation in turbulent flow: Measurement and modeling of particle size distributions. Journal (American Water Works Association), 82(8, CONSTRUCTION), 54-68.

Chan, F., Pennock, W., Niu, M., Lion, L.W. (2014) On the Invertibility of Almost Everywhere Left-Standard Algebras. *International Journal of Advanced Computer Technology*, 1-10. http://thatsmathematics.com/mathgen/paper.php

Cleasby, J.L. (1984). Is Velocity Gradient a Valid Turbulent Flocculation Parameter? Journal of Environmental Engineering - ASCE, 110:5:875.

Kumar, J., Warnecke, G., Peglow, M., & Heinrich, S. (2009). Comparison of numerical methods for solving population balance equations incorporating aggregation and breakage. *Powder Technology,* 218-229.

PID Theory Explained. (2011, March 29). Retrieved November 8, 2014, from http://www.ni.com/white-paper/3782/en/

Smoluchowski, M. (1917). Versuch Einer Mathematischen Theorie der Koagulations-kinetic Killoider Losungen. *Zeitschrift Fur Physikalische Chemie, 92*(2).

Valioulis, I., & List, E. (1981). Numerical simulation of a sedimentation basin. 1. Model development. *Environmental Science & Technology,* 242-247.

Weber-Shirk, M.L *Flocculation model* [PowerPoint slides] https://confluence.cornell.edu/display/cee4540/syllabus